Steady detonation waves via the Boltzmann equation for a reacting mixture

2003 J. Phys. A: Math. Gen. 36 5381

(http://iopscience.iop.org/0305-4470/36/20/303)

INSTITUTE OF PHYSICS PUBLISHING JOURNAL OF PHYSICS A: MATHEMATICAL AND GENERAL

J. Phys. A: Math. Gen. **36** (2003) 5381–5398 PII: S0305-4470(03)53628-9

Steady detonation waves via the Boltzmann equation for a reacting mixture

F Conforto[1], R Monaco[2], F Schürrer[3] and I Ziegler[3]

[1] Dipartimento di Matematica, Università di Messina, Italy
[2] Dipartimento di Matematica, Politecnico di Torino, Italy
[3] Institut für Theoretische Physik, Technische Universität Graz, Austria

Received 17 September 2002, in final form 28 February 2003
Published 7 May 2003
Online at stacks.iop.org/JPhysA/36/5381

Abstract

Based on the Boltzmann equation, the detonation problem is dealt with on a mesoscopic level. The model is based on the assumption that ahead of a shock an explosive gas mixture is in meta stable equilibrium. Starting from the Von Neumann point the chemical reaction, initiated by the pressure jump, proceeds until the chemical equilibrium is reached. Numerical solutions of the derived macroscopic equations as well as the corresponding Hugoniot diagrams which reveal the physical relevance of the mathematical model are provided.

PACS numbers: 47.40.−x, 82.40.Fp

1. Introduction

Detonation is a rapid and violent process of combustion generating a strong shock wave which is sustained by chemical reactions. The most easily measurable characteristic quantity of a detonation is the velocity at which the shock propagates into the explosive gas mixture. The front of a detonation wave has approximately a plane shape and moves with constant supersonic velocity. According to such a scheme, it is reasonable, on mathematical grounds, to treat detonation as a one-dimensional steady propagation problem of a shock front moving with constant velocity $\mathcal{D}$ (see [1, 2]). Referring to figure 1, where the pressure of the gas is plotted versus space, the steady detonation process can be represented (as discussed in [3, 4]) in the following way.

(i) In region $D_1 = [x_0, +\infty)$, ahead of the shock, an explosive mixture is in metastable equilibrium at rest with negligible reaction rate.
(ii) At the space point x_0 there is a jump discontinuity. Until this discontinuity (*Von Neumann point*) no reaction takes place. Starting from this point, the chemical reaction (in general an exothermic reaction) is initiated by the pressure jump, so that the reaction itself proceeds with a finite reaction rate and is completed in the *final state point* x_F, where the gas mixture

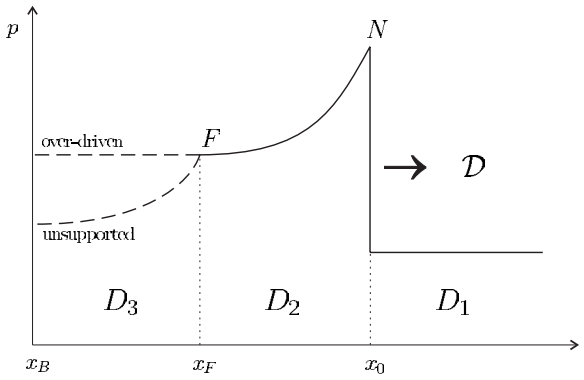

Figure 1. Qualitative evolution of the pressure p during a detonation process caused by a shock wave of speed $\mathcal{D}$; D_1 denotes the region ahead of the shock, D_2 the chemical reaction zone and D_3 the following flow zone; N indicates the Von Neumann point at x_0, F the final state point at x_F and x_B the rear boundary point.

reaches chemical equilibrium. Hereinafter, we will indicate with $D_2 = (x_F, x_0)$ such a region, the so-called *reaction zone*, characterized by strong chemical disequilibrium. The flow in the reaction zone is steady and the shock front propagates with constant detonation velocity $\mathcal{D}$.

(iii) In region $D_3 = [x_B, x_F]$, the gas mixture is in chemical equilibrium. Region D_3 is known in the literature as the *following flow* connecting the rear boundary point x_B to the final state point x_F. Such a rear boundary can be interpreted as the side of a hypothetical piston moving with constant velocity u_p. In region D_3, the pressure profile can be characterized either by a constant state up to the point x_F (*over-driven detonation*), or by a constant state followed by a rarefaction wave which takes its origin in x_F itself (*unsupported detonation*).

According to this phenomenology, it is possible to state two mathematical problems.

(a) Solving the shock wave problem between the point $x_0 \in D_1$ and any point $x_R \in D_2$, is achieved by finding all possible steady solutions for the reaction zone and by treating $\mathcal{D}$ as a parameter once the physical state of the explosive mixture in D_1 has been stated. The solution of such a problem provides then the thickness $|x_0 - x_F|$ of the reaction zone. This problem is known in the literature as the $\mathcal{D}$*-discussion* [4].

(b) Determining a value of $\mathcal{D}$ leads to a suitable steady solution for a given piston velocity u_p which in turn allows the evaluation of the flow in D_3. This problem is generally quoted as the *piston problem*.

The two problems are obviously related since problem (a) determines the existence of steady solutions for all values of $\mathcal{D}$ above a certain minimum value. For such a value, the following flow is characterized by an unsupported detonation; higher values of $\mathcal{D}$ allow over-driven detonations, so that a solution of problem (b) depends on a solution of problem (a).

These problems have been widely studied in the literature, starting from the so-called ZND model [4] which is still considered as the simplest description of the steady detonation for an explosive mixture with only a one-way exothermic reaction. The following papers [5–15] take into account state equations of detonating mixtures at a macroscopic level. In particular, [7, 10, 11] consider macroscopic equations at a Euler level, while the others

include in the equations viscous and/or diffusion terms. Moreover, [9, 11, 12, 15] are also concerned with the problem of nonlinear stability of the travelling wave. Finally, [14] deals with detonation initiation. In order to get acquainted with the mathematical models used by the aforementioned authors, we recommend the book [16]. Nevertheless, the papers [5–15] do not provide the profiles of macroscopic quantities relevant to the process in the reaction zone $[x_F, x_0]$. However, a detailed study of these profiles can be found in two very recent papers [17, 18] based on Monte Carlo simulations. In addition, a deep analysis of the profiles in the reaction zone and conditions for overdriven or unsupported detonations are presented in [19, 20], where the main objective is the study of linear and nonlinear stabilities for the detonation processes considered in [20]. At the end of the paper, in section 7, we will give some more details about the results of these last four papers.

In the present paper, the general procedure used to study the detonation problem is different from those above. We start with the Boltzmann equation for a gas mixture of four components undergoing a reversible bimolecular reaction $1 + 2 \rightleftharpoons 3 + 4$, very often considered in [1, 2, 4], as a characteristic of several detonation processes. The actual explicit expression of the reaction rate at the kinetic level is provided. Let us stress that knowledge of the reaction rate is important since this quantity decides whether a detonation does or does not occur (see [1], p 224, and related bibliography). We then derive a set of macroscopic equations at a Euler level and provide the mathematical formulation of the above problem (a), proposing its solution procedure and determining the detonation wave structure. In the authors' opinion such a procedure, involving also the phenomenology of detonation at the microscopic level, is more complete and detailed. The fact that we consider a special chemical reaction (bimolecular) does not restrict the generality of the procedure proposed here. Other types of chemical reactions require a different Boltzmann model at the kinetic level and different expressions for the reaction rate but do not affect the mathematical structure of the macroscopic equations and the problem presented here.

An analogous philosophy to treat detonation problems has been proposed for the first time in recent papers [21, 22]. In these papers, the microscopic state of the mixture has been described in terms of very simple discrete velocity models, taking into account both bimolecular and three-molecular reactions coming from the hydrogen–oxygen chain. However, these models provide only heuristic expressions for the reaction rates. Using these last models the problem of linear stability has been investigated in [23]. The plan of the present paper is organized as follows. In section 2 we resume the relevant features of the kinetic model deduced in a very recent work [24]. We deduce the macroscopic equations and compute the reaction rate on the basis of a cross section model for exothermic reactions proposed in [25] in section 3. In section 4, we perform the solution procedure for the mathematical problem (a) which allows us to determine all the states of the reaction zone and its thickness once a boundary value problem, involving a nonlinear ordinary differential equation, is solved. Moreover, in section 5, we provide the procedure to draw the Hugoniot diagram which describes, depending on the parameter $\mathcal{D}$, all the detonation states. We estimate as well the so-called Chapman–Jouguet velocity $\mathcal{D}_J$ [4], relevant for solving problem (b). Finally, in section 6, numerical results showing detonation profiles and Hugoniot diagrams will be proposed in order to evaluate the thickness of the reaction zone.

Let us emphasize that the procedure proposed here deals with macroscopic equations closed at a Euler level. Future developments could involve macroscopic equations including viscous and diffusion terms, equations coming from a semi-continuous Boltzmann model [26] or from kinetic models of dense fluids, as discussed in a very recent review [27].

2. The kinetic model

Consider a mixture of four gases, say 1, 2, 3 and 4, undergoing a bimolecular chemical reversible reaction

$$1 + 2 \rightleftharpoons 3 + 4. \tag{1}$$

Examples of this type of reactions triggering detonation are

$$H_2O + H \rightleftharpoons OH + H_2 \qquad CO_2 + H_2 \rightleftharpoons CO + H_2O \qquad O + N_2 \rightleftharpoons NO + N.$$

The microscopic state of the gas is defined by the one-particle distribution functions f_i for each gas species, $i = 1, \ldots, 4$, where

$$f_i = f_i(t, \mathbf{x}, \mathbf{v}) \qquad t \in \mathbb{R}^+ \quad \mathbf{x} \in \mathbb{R}^3 \quad \mathbf{v} \in \mathbb{R}^3.$$

Unless necessary, hereinafter the explicit dependence of f_i on time t and position $\mathbf{x}$ will be often omitted. Each gas particle is characterized by its mass m_i and its internal chemical bond energy E_i. These quantities will be used in the following:

$$r_i = \frac{m_i}{M} \qquad M = m_1 + m_2 \qquad \text{and} \qquad E = E_3 + E_4 - E_1 - E_2$$

where $E \geqslant 0$. Because of mass conservation of reaction (1), $M = m_3 + m_4$. Let us indicate with V and V' the relative speeds of particles before and after collisions, and by $\boldsymbol{\Omega}$ and $\boldsymbol{\Omega}'$ the unit vectors defining their directions. When defining other quantities appearing in the kinetic equations, it is preferable to distinguish between elastic and inelastic collisions.

The elastic collisions are all those between possible pairs $(i, j), i, j = 1, \ldots, 4$, of particle species which preserve mass, momentum and kinetic energy. The post-collisional velocities, computed according to these conservation laws, are given by

$$\mathbf{v}_{ij} = \frac{m_i\mathbf{v} + m_j\mathbf{w} - m_jV\boldsymbol{\Omega}'}{m_i + m_j} \qquad \mathbf{w}_{ij} = \frac{m_i\mathbf{v} + m_j\mathbf{w} + m_iV\boldsymbol{\Omega}'}{m_i + m_j}. \tag{2}$$

The elastic mechanism is ruled by a differential scattering cross section, which in general depends upon the relative speed of colliding particles and the scalar product $\boldsymbol{\Omega} \cdot \boldsymbol{\Omega}'$. This quantity will be indicated by $I_{ij}^{ij} = I_{ij}^{ij}(V, \boldsymbol{\Omega}, \boldsymbol{\Omega}')$ with the property that $I_{ij}^{ij} = I_{ji}^{ji}$.

The chemical reactions are inelastic collisions of the pair of particles $(1, 2)$ which produce the other pair $(3, 4)$ and vice versa. These interactions preserve mass, momentum and total (kinetic plus chemical bond) energy. Nevertheless, since $E \geqslant 0$, production of particles $(3, 4)$ requires that the kinetic energy of the pair $(1, 2)$ must exceed an assigned quantity (endothermic reaction), while reaction $(3, 4) \to (1, 2)$ is the exothermic one. Introducing the quantities

$$\mu_{ij} = \frac{m_im_j}{M} \qquad \epsilon_{ij}^2 = \frac{2E}{\mu_{ij}} \qquad i, j = 1, \ldots, 4 \tag{3}$$

as well as

$$V_{12} = \left[\frac{\mu_{12}}{\mu_{34}}\left(V^2 - \epsilon_{12}^2\right)\right]^{\frac{1}{2}} \qquad V_{34} = \left[\frac{\mu_{34}}{\mu_{12}}\left(V^2 + \epsilon_{34}^2\right)\right]^{\frac{1}{2}} \tag{4}$$

and taking into account the conservation laws, it is possible to compute the outcoming velocities, $(\mathbf{v}_1, \mathbf{w}_1)$ or $(\mathbf{v}_2, \mathbf{w}_2)$, of the interaction $(1, 2) \to (3, 4)$ in terms of the incoming velocities

$$\begin{aligned} \mathbf{v}_1 &= r_1\mathbf{v} + r_2\mathbf{w} - r_4V_{12}\boldsymbol{\Omega}' \qquad & \mathbf{w}_1 &= r_1\mathbf{v} + r_2\mathbf{w} + r_3V_{12}\boldsymbol{\Omega}' \\ \mathbf{v}_2 &= r_2\mathbf{v} + r_1\mathbf{w} - r_3V_{12}\boldsymbol{\Omega}' \qquad & \mathbf{w}_2 &= r_2\mathbf{v} + r_1\mathbf{w} + r_4V_{12}\boldsymbol{\Omega}'. \end{aligned} \tag{5}$$

Analogously, the outcoming velocities, $(\mathbf{v}_3, \mathbf{w}_3)$ or $(\mathbf{v}_4, \mathbf{w}_4)$, of the interaction $(3, 4) \to (1, 2)$ are provided by

$$\begin{aligned} \mathbf{v}_3 &= r_3\mathbf{v} + r_4\mathbf{w} - r_2 V_{34}\boldsymbol{\Omega}' \qquad & \mathbf{w}_3 &= r_3\mathbf{v} + r_4\mathbf{w} + r_1 V_{34}\boldsymbol{\Omega}' \\ \mathbf{v}_4 &= r_4\mathbf{v} + r_3\mathbf{w} - r_1 V_{34}\boldsymbol{\Omega}' \qquad & \mathbf{w}_4 &= r_4\mathbf{v} + r_3\mathbf{w} + r_2 V_{34}\boldsymbol{\Omega}'. \end{aligned} \tag{6}$$

The inelastic mechanism of interaction, similar to the elastic one, is ruled by the differential cross section I_{12}^{34} for reaction $(1, 2) \to (3, 4)$ and I_{34}^{12} for reaction $(3, 4) \to (1, 2)$. These quantities are again functions of V, $\boldsymbol{\Omega}$ and $\boldsymbol{\Omega}'$ and are related by the detailed balance condition [28] given by

$$\mu_{34}^2 V^2 I_{34}^{12}(V, \boldsymbol{\Omega}, \boldsymbol{\Omega}') = \mu_{12}^2 V_{34}^2 I_{12}^{34}(V_{34}, \boldsymbol{\Omega}, \boldsymbol{\Omega}'). \tag{7}$$

Moreover, recall that inelastic differential cross sections satisfy the property $I_{ij}^{hk} = I_{ji}^{kh}$.

In the present paper, for the exothermic reaction we choose the cross section proposed in [25],

$$I_{34}^{12}(V) = \frac{\beta}{V}\left(1 - \frac{\chi^2}{V^2}\right) U(V - \chi) \tag{8}$$

where χ denotes a threshold velocity, β is a scale factor and U is the Heaviside function. This synthetic cross section for exothermic chemical reactions represents the main features of realistic chemical cross sections [29]. It includes the necessary activation threshold and decreases monotonically for high energies. It can be considered as an improved line-of-centre cross section. Line-of-centre cross sections were suggested in [30] and have been used in several papers as, e.g., in [31]. Applying the conditions of detailed balance, we obtain the endothermic cross section

$$I_{12}^{34}(V) = \beta\left(\frac{\mu_{34}}{\mu_{12}}\right)^{\frac{3}{2}} \frac{\sqrt{V^2 - \epsilon_{12}^2}}{V^2}\left(1 - \frac{\chi^2}{\frac{\mu_{12}}{\mu_{34}}\left(V^2 - \epsilon_{12}^2\right)}\right) U\left(V - \sqrt{\frac{\mu_{34}}{\mu_{12}}\chi^2 + \epsilon_{12}^2}\right). \tag{9}$$

The kinetic equations (Boltzmann equation) for the reactive gas mixture, which rule the spatio-temporal evolution of the system, are given by

$$\frac{\partial f_i}{\partial t} + \mathbf{v} \cdot \nabla f_i = Q_i[\mathbf{f}] + \mathcal{R}_i[\mathbf{f}] \qquad i = 1, \ldots, 4 \tag{10}$$

where $\mathbf{f} = \{f_1, f_2, f_3, f_4\}(t, \mathbf{x}, \mathbf{v})$. In equation (10) the quantities Q_i and $\mathcal{R}_i$ are the collision terms due to elastic and inelastic collisions. All these quantities are functions of $(t, \mathbf{x}, \mathbf{v})$ as well.

The elastic collision terms are well known in the literature when one considers the full Boltzmann equation extended to a mixture of four inert gases [32, 33]:

$$\begin{aligned} Q_i[\mathbf{f}] = \sum_j \int_{\mathbb{R}^3} \mathrm{d}\mathbf{w} \int_{\mathcal{S}} V I_{ij}^{ij}(V, \boldsymbol{\Omega}, \boldsymbol{\Omega}') f_i(\mathbf{v}_{ij}) f_j(\mathbf{w}_{ij})\, \mathrm{d}\boldsymbol{\Omega}' \\ - f_i(\mathbf{v}) \sum_j \int_{\mathbb{R}^3} \mathrm{d}\mathbf{w} \int_{\mathcal{S}} V I_{ij}^{ij}(V, \boldsymbol{\Omega}, \boldsymbol{\Omega}') f_j(\mathbf{w})\, \mathrm{d}\boldsymbol{\Omega}'. \end{aligned} \tag{11}$$

Here $\mathbf{v}_{ij}$ and $\mathbf{w}_{ij}$, $i, j = 1, \ldots, 4$, are given by equations (2) and $\mathcal{S}$ is the unit sphere. The inelastic collision terms have been derived in [24]. For more precise description of these terms the reader can refer to [34]. In particular, we have

$$\begin{aligned} \mathcal{R}_1[\mathbf{f}] = \left(\frac{\mu_{12}}{\mu_{34}}\right)^3 \int_{\mathbb{R}^3} \mathrm{d}\mathbf{w} \int_{\mathcal{S}} V I_{12}^{34}(V, \boldsymbol{\Omega}, \boldsymbol{\Omega}') f_3(\mathbf{v}_1) f_4(\mathbf{w}_1)\, \mathrm{d}\boldsymbol{\Omega}' \\ - f_1(\mathbf{v}) \int_{\mathbb{R}^3} \mathrm{d}\mathbf{w} \int_{\mathcal{S}} V I_{12}^{34}(V, \boldsymbol{\Omega}, \boldsymbol{\Omega}') f_2(\mathbf{w})\, \mathrm{d}\boldsymbol{\Omega}' \end{aligned} \tag{12a}$$

$$\mathcal{R}_2[\mathbf{f}] = \left(\frac{\mu_{12}}{\mu_{34}}\right)^3 \int_{\mathbb{R}^3} \mathrm{d}\mathbf{w} \int_{\mathcal{S}} V I_{12}^{34}(V, \boldsymbol{\Omega}, \boldsymbol{\Omega}') f_4(\mathbf{v}_2) f_3(\mathbf{w}_2)\, \mathrm{d}\boldsymbol{\Omega}' - f_2(\mathbf{v}) \int_{\mathbb{R}^3} \mathrm{d}\mathbf{w} \int_{\mathcal{S}} V I_{12}^{34}(V, \boldsymbol{\Omega}, \boldsymbol{\Omega}') f_1(\mathbf{w})\, \mathrm{d}\boldsymbol{\Omega}' \tag{12b}$$

$$\mathcal{R}_3[\mathbf{f}] = \left(\frac{\mu_{34}}{\mu_{12}}\right)^3 \int_{\mathbb{R}^3} \mathrm{d}\mathbf{w} \int_{\mathcal{S}} V I_{34}^{12}(V, \boldsymbol{\Omega}, \boldsymbol{\Omega}') f_1(\mathbf{v}_3) f_2(\mathbf{w}_3)\, \mathrm{d}\boldsymbol{\Omega}' - f_3(\mathbf{v}) \int_{\mathbb{R}^3} \mathrm{d}\mathbf{w} \int_{\mathcal{S}} V I_{34}^{12}(V, \boldsymbol{\Omega}, \boldsymbol{\Omega}') f_4(\mathbf{w})\, \mathrm{d}\boldsymbol{\Omega}' \tag{12c}$$

$$\mathcal{R}_4[\mathbf{f}] = \left(\frac{\mu_{34}}{\mu_{12}}\right)^3 \int_{\mathbb{R}^3} \mathrm{d}\mathbf{w} \int_{\mathcal{S}} V I_{34}^{12}(V, \boldsymbol{\Omega}, \boldsymbol{\Omega}') f_2(\mathbf{v}_4) f_1(\mathbf{w}_4)\, \mathrm{d}\boldsymbol{\Omega}' - f_4(\mathbf{v}) \int_{\mathbb{R}^3} \mathrm{d}\mathbf{w} \int_{\mathcal{S}} V I_{34}^{12}(V, \boldsymbol{\Omega}, \boldsymbol{\Omega}') f_3(\mathbf{w})\, \mathrm{d}\boldsymbol{\Omega}' \tag{12d}$$

where $\mathbf{v}_i$ and $\mathbf{w}_i$, $i = 1, \ldots, 4$, are defined by equations (5) and (6).

According to [24], we now recall the principal properties of the collision terms (11) and (12). Conservation laws of mass, momentum and total energy imply

$$\sum_{i=1}^{4} \int_{\mathbb{R}^3} \psi_i(\mathbf{v}) \{Q_i[\mathbf{f}] + \mathcal{R}_i[\mathbf{f}]\}(\mathbf{v})\, \mathrm{d}\mathbf{v} = 0 \tag{13}$$

when $\psi_i = m_i$, or $\psi_i = m_i \mathbf{v}$, or $\psi_i = E_i + m_i v^2/2$, $i = 1, \ldots, 4$. Moreover, only for the reactive collision terms mass conservation results in

$$\int_{\mathbb{R}^3} \{\mathcal{R}_1[\mathbf{f}]\}(\mathbf{v})\, \mathrm{d}\mathbf{v} = \int_{\mathbb{R}^3} \{\mathcal{R}_2[\mathbf{f}]\}(\mathbf{v})\, \mathrm{d}\mathbf{v} = -\int_{\mathbb{R}^3} \{\mathcal{R}_3[\mathbf{f}]\}(\mathbf{v})\, \mathrm{d}\mathbf{v} = -\int_{\mathbb{R}^3} \{\mathcal{R}_4[\mathbf{f}]\}(\mathbf{v})\, \mathrm{d}\mathbf{v}. \tag{14}$$

Kinetic equations (10) provide an *H*-theorem. Without going into detail (see again [24]) let us recall that equations (10) admit a stable equilibrium solution if and only if

$$Q_i[\mathbf{f}] = \mathcal{R}_i[\mathbf{f}] = 0 \qquad i = 1, \ldots, 4 \quad \forall \mathbf{v}. \tag{15a}$$

In particular, $Q_i[\mathbf{f}] = 0 \Longrightarrow$

$$f_i(\mathbf{v}) f_j(\mathbf{w}) = f_i(\mathbf{v}_{ij}) f_j(\mathbf{w}_{ij}) \qquad i, j = 1, \ldots, 4 \quad \forall \mathbf{v}, \mathbf{w}, \boldsymbol{\Omega}' \tag{15b}$$

while $\mathcal{R}_i[\mathbf{f}] = 0 \Longrightarrow$

$$\begin{cases} f_i(\mathbf{v}) f_j(\mathbf{w}) = f_i(\mathbf{v}_{ij}) f_j(\mathbf{w}_{ij}) \\ (m_3 m_4)^3 f_1(\mathbf{v}) f_2(\mathbf{w}) = (m_1 m_2)^3 f_3(\mathbf{v}_1) f_4(\mathbf{w}_1) \end{cases} \tag{15c}$$

$i, j = 1, \ldots, 4$, and $\forall \mathbf{v}, \mathbf{w}, \boldsymbol{\Omega}'$. Condition (15*b*) implies (see [32])

$$f_i(\mathbf{v}) = \tilde{f}_i(\mathbf{v}) = n_i \left(\frac{m_i}{2\pi\kappa T}\right)^{\frac{3}{2}} \exp\left(-\frac{m_i(\mathbf{v} - \mathbf{u})^2}{2\kappa T}\right) \tag{16}$$

whereas conditions (15*c*) are satisfied if the distribution functions have the form of equation (16) with the further constraint

$$\frac{n_1 n_2}{n_3 n_4} = \left(\frac{m_1 m_2}{m_3 m_4}\right)^{\frac{3}{2}} \exp\left(\frac{E}{\kappa T}\right) \tag{17}$$

κ being the Boltzmann constant.

Equation (16) provides the well-known expressions of Maxwellian distribution functions, governing equilibrium for elastic scattering only. In general, the $\tilde{f}_i$ are functions of $(t, \mathbf{x}, \mathbf{v})$ (*local Maxwellians*) through the number densities n_i, the mean velocity $\mathbf{u}$ and the temperature T defined as follows:

$$n_i(t,\mathbf{x}) = \int_{\mathbb{R}^3} f_i(t,\mathbf{x},\mathbf{v})\,\mathrm{d}\mathbf{v} \qquad n(t,\mathbf{x}) = \sum_i n_i(t,\mathbf{x}) \tag{18}$$

$$\mathbf{u}(t,\mathbf{x}) = \frac{1}{\rho(t,\mathbf{x})}\sum_i m_i \int_{\mathbb{R}^3} \mathbf{v} f_i(t,\mathbf{x},\mathbf{v})\,\mathrm{d}\mathbf{v} \qquad \rho(t,\mathbf{x}) = \sum_i m_i n_i(t,\mathbf{x}) \tag{19}$$

$$T(t,\mathbf{x}) = \frac{1}{3\kappa n(t,\mathbf{x})}\sum_i m_i \int_{\mathbb{R}^3} [\mathbf{v}-\mathbf{u}(t,\mathbf{x})]^2 f_i(t,\mathbf{x},\mathbf{v})\,\mathrm{d}\mathbf{v} \tag{20}$$

where n and ρ are the total number and mass density, respectively.

Equation (17) expresses the *mass action law* of chemical equilibrium [35]. Therefore, when only equation (16) holds, the gas is in mechanical equilibrium and equation (15*b*) is satisfied; when equations (16) and (17) simultaneously hold then mechanical–chemical equilibrium is reached and all the right-hand sides of the kinetic equations (10) vanish.

3. Macroscopic equations

The procedure to obtain macroscopic equations from the kinetic equations is well known [36]. In the present case, the balance equation for the particle number density of each species is obtained by integrating equations (10) over $\mathbf{v}$

$$\frac{\partial n_i}{\partial t} + \nabla\cdot(n_i\mathbf{u}_i) = \int_{\mathbb{R}^3} \mathcal{R}_i[\mathbf{f}]\,\mathrm{d}\mathbf{v} \stackrel{\text{def}}{=} S_i. \tag{21}$$

By multiplying equations (10) by $m_i\mathbf{v}$, summing over i (taking into account the properties (13)), and integrating over $\mathbf{v}$, we obtain the conservation equation of momentum

$$\frac{\partial}{\partial t}(\rho\mathbf{u}) + \nabla\cdot(\rho\mathbf{u}\otimes\mathbf{u} + P) = \mathbf{0} \tag{22}$$

where

$$P(t,\mathbf{x}) = \sum_i m_i \int_{\mathbb{R}^3} [\mathbf{v}-\mathbf{u}(t,\mathbf{x})]\otimes[\mathbf{v}-\mathbf{u}(t,\mathbf{x})] f_i(t,\mathbf{x},\mathbf{v})\,\mathrm{d}\mathbf{v}. \tag{23}$$

Finally, the balance of total energy is achieved by multiplying equations (10) by $\frac{1}{2}m_i v^2 + E_i$, summing over i (taking into account the properties (13) and (14)) and integrating over $\mathbf{v}$:

$$\frac{\partial}{\partial t}\left(\mathcal{E} + \rho\frac{u^2}{2} + \mathcal{E}_{ch}\right) + \nabla\cdot\left(\left[\left(\mathcal{E} + \rho\frac{u^2}{2} + \mathcal{E}_{ch}\right)I + P\right]\mathbf{u} + \mathbf{q} + \mathbf{q}_{ch}\right) = 0 \tag{24}$$

where I is the unit tensor and

$$\mathcal{E}(t,\mathbf{x}) = \frac{3}{2}n(t,\mathbf{x})\kappa T(t,\mathbf{x}) = \frac{1}{2}\,\mathrm{tr}[P(t,\mathbf{x})] \qquad \mathcal{E}_{ch}(t,\mathbf{x}) = \sum_i E_i n_i(t,\mathbf{x}) \tag{25}$$

$$\mathbf{q}(t,\mathbf{x}) = \frac{1}{2}\sum_i m_i \int_{\mathbb{R}^3} [\mathbf{v}-\mathbf{u}(t,\mathbf{x})]^2[\mathbf{v}-\mathbf{u}(t,\mathbf{x})] f_i(t,\mathbf{x},\mathbf{v})\,\mathrm{d}\mathbf{v} \tag{26}$$

$$\mathbf{q}_{ch}(t,\mathbf{x}) = \sum_i E_i\left[\int_{\mathbb{R}^3} \mathbf{v} f_i(t,\mathbf{x},\mathbf{v})\,\mathrm{d}\mathbf{v} - n_i(t,\mathbf{x})\mathbf{u}(t,\mathbf{x})\right]. \tag{27}$$

Equations (21), (22) and (24) are the macroscopic equations which are known as a non-closed set of equations. The simplest way to provide a closure is to assume that the distribution functions appearing in equations (10) are local Maxwellians with number densities n_i which do not necessarily satisfy the mass action law (17). This assumption reflects the fact that the gas has reached mechanical equilibrium but can still be in chemical non-equilibrium. As we shall see, such a physical picture is consistent with the purposes of the present paper. Accordingly, when $f_i = \tilde{f}_i$, it is possible to show that $\mathbf{q}$ and $\mathbf{q}_{ch}$ vanish, and the tensor P becomes diagonal, so that closure of the above set is performed.

In a more direct and rigorous way, we can derive the closed set of spatially one-dimensional macroscopic equations with the following procedure.

(a) Inserting local Maxwellians (given by equation (16)) into the kinetic equations (10) and computing explicitly the time and space derivatives of the macroscopic observables $n_i(t, \mathbf{x})$, $\mathbf{u}(t, \mathbf{x})$ and $T(t, \mathbf{x})$, results in

$$\begin{aligned}\left(\frac{m_i}{2\pi\kappa T}\right)^{\frac{3}{2}} \exp\left[-\frac{m_i(v-u)^2}{2\kappa T}\right]\left\{\frac{\partial n_i}{\partial t} + \left[\frac{n_i m_i (v-u)^2}{2\kappa T^2} - \frac{3n_i}{2T}\right]\frac{\partial T}{\partial t} + \frac{n_i m_i (v-u)}{\kappa T}\frac{\partial u}{\partial t}\right\} \\ + v\left(\frac{m_i}{2\pi\kappa T}\right)^{\frac{3}{2}} \exp\left[-\frac{m_i(v-u)^2}{2\kappa T}\right] \\ \times \left\{\frac{\partial n_i}{\partial x} + \left[\frac{n_i m_i (v-u)^2}{2\kappa T^2} - \frac{3n_i}{2T}\right]\frac{\partial T}{\partial x} + \frac{n_i m_i (v-u)}{\kappa T}\frac{\partial u}{\partial x}\right\} \\ = \mathcal{R}_i[\tilde{f}_1, \tilde{f}_2, \tilde{f}_3, \tilde{f}_4]. \qquad (28)\end{aligned}$$

(b) Performing the same procedure on equation (28) which had been applied to obtain equations (21), (22) and (24), namely multiplying equation (28) by 1, $m_i\mathbf{v}$ and $\frac{1}{2}m_i v^2 + E_i$, respectively, summing up over i (in the last two cases) and integrating over $\mathbf{v}$ leads to

$$\frac{\partial n_i}{\partial t} + \frac{\partial}{\partial x}(n_i u) = S_i \qquad i = 1, \ldots, 4 \qquad (29)$$

$$\frac{\partial}{\partial t}\left[u\sum_i m_i n_i\right] + \frac{\partial}{\partial x}\left[u^2\sum_i m_i n_i + \kappa T\sum_i n_i\right] = 0 \qquad (30)$$

$$\begin{aligned}\frac{\partial}{\partial t}\left[u^2\sum_i m_i n_i + 3\kappa T\sum_i n_i + 2\sum_i E_i n_i\right] \\ + \frac{\partial}{\partial x}\left[u\left(u^2\sum_i m_i n_i + 5\kappa T\sum_i n_i + 2\sum_i E_i n_i\right)\right] = 0 \qquad (31)\end{aligned}$$

which represents a closed set of six macroscopic equations in the unknowns n_i, u and T.

Once again we emphasize that the last equations represent the spatio-temporal relaxation of the physical state of a reacting gas mixture in mechanical equilibrium to chemical equilibrium. Finally, let us note that the quantities S_i, appearing in equations (21) and (29), are expressed by

$$S_i = \lambda_i S_1 \qquad \begin{cases}\lambda_i = 1 & \text{for} \quad i = 1, 2 \\ \lambda_i = -1 & \text{for} \quad i = 3, 4\end{cases}$$

where

$$S_1 = \left(\frac{\mu_{12}}{\mu_{34}}\right)^3 \frac{n_3 n_4}{(2\pi\kappa T)^3}(m_3 m_4)^{\frac{3}{2}} \int_{\mathbb{R}^3} \mathrm{d}\mathbf{v} \int_{\mathbb{R}^3} \mathrm{d}\mathbf{w} \times \int_{\mathcal{S}} V I_{12}^{34}(V, \boldsymbol{\Omega}, \boldsymbol{\Omega}') \exp\left[-\frac{m_3(\mathbf{v}_1 - \mathbf{u})^2 + m_4(\mathbf{w}_1 - \mathbf{u})^2}{2\kappa T}\right] \mathrm{d}\boldsymbol{\Omega}' - \frac{n_1 n_2}{(2\pi\kappa T)^3}(m_1 m_2)^{3/2} \int_{\mathbb{R}^3} \mathrm{d}\mathbf{v} \int_{\mathbb{R}^3} \mathrm{d}\mathbf{w} \times \int_{\mathcal{S}} V I_{12}^{34}(V, \boldsymbol{\Omega}, \boldsymbol{\Omega}') \exp\left[-\frac{m_1(\mathbf{v} - \mathbf{u})^2 + m_2(\mathbf{w} - \mathbf{u})^2}{2\kappa T}\right] \mathrm{d}\boldsymbol{\Omega}'. \tag{32}$$

Now, if the endothermic cross section I_{12}^{34}, equation (9), is inserted into equation (32), and the integrals are explicitly computed, we obtain, after rather cumbersome calculations, the reaction rate

$$S_1(n_1, \ldots, n_4, T) = -4\pi\beta\frac{\mu_{34}}{\kappa T}\left[n_1 n_2 \left(\frac{m_3 m_4}{m_1 m_2}\right)^{\frac{3}{2}} \exp\left[-\frac{E}{\kappa T}\right] - n_3 n_4\right] \times \left\{\frac{\chi}{\pi}\sqrt{\frac{2\pi\kappa T}{\mu_{34}}} \exp\left[-\frac{\mu_{34}\chi^2}{2\kappa T}\right] + \left(\frac{\kappa T}{\mu_{34}} - \chi^2\right)\left[1 - \operatorname{erf}\left(\sqrt{\frac{\mu_{34}}{2\kappa T}}\chi\right)\right]\right\}. \tag{33}$$

Equations (29)–(31), with S_1 expressed by equation (33), represent the set of equations describing the physical state of the detonation process in the three regions D_1, D_2 and D_3.

4. Analysis and solution of the detonation problem

According to the physical phenomenology presented in the introduction, the analysis of the detonation problem will be carried out by assuming that:

(1) In the reaction zone the gas mixture is in chemical non-equilibrium but in mechanical equilibrium. Indeed, the macroscopic equations (29)–(31) represent such a physical situation.
(2) Since detonation is initiated by the exothermic reaction $3 + 4 \rightarrow 1 + 2$, hereinafter the number density of the 'second' gas component, namely n_2, is assumed as the progress variable of the chemical production process.

Assumption (1) seems to be physically consistent since the typical time of elastic relaxation is several orders of magnitude shorter than that of chemical relaxation.

Since we are searching for steady solutions to the detonation problem, let us change our frame from laboratory coordinates to steady ones attached to the shock wave moving with constant velocity $\mathcal{D}$ through the transformation

$$z = x - \mathcal{D}t. \tag{34}$$

Consequently, we have $\partial/\partial t = -\mathcal{D}\,\mathrm{d}/\mathrm{d}z$ and $\partial/\partial x = \mathrm{d}/\mathrm{d}z$. Let us then indicate with $z_0 \equiv x_0^+ - \mathcal{D}t$ and $z_N \equiv x_0^- - \mathcal{D}t$ the downstream and upstream (Von Neumann point) coordinates of the shock jump, respectively. In the same fashion, we will denote the coordinate of the final point of the reaction zone with z_F. Moreover, keeping in mind the macroscopic equations (29)–(31), we can now characterize the physical states of the two regions D_1 and D_2.

(a) In region $D_1 = [z_0, +\infty)$, where the mixture is at rest in absolute equilibrium and with negligible reaction rate, the physical state is given by

$$\begin{cases} n_i(z) = n_{i0} \\ u(z) = 0 \\ T(z) = T_0 \\ S_1(z) = 0 \end{cases} \qquad \forall z \in D_1. \tag{35}$$

(b) In region $D_2 = (z_F, z_N)$, the state variables $n_1(z), \ldots, n_4(z)$, $u(z)$ and $T(z)$ change their values under the influence of chemical disequilibrium ($S_1(z) \neq 0$). At the extrema of D_2, the physical state is characterized by

$$\begin{cases} n_2 = n_{20} & \text{for} \quad z = z_N \\ S_1 = 0 & \text{for} \quad z = z_F \end{cases} \tag{36}$$

since in z_N the reaction starts and n_2 is assumed to have still the same value as in D_1, while in z_F the chemical reaction is completed and the reaction rate vanishes.

We now apply transformation (34) to the macroscopic equations (29)–(31) and use property (14) (conservation of mass species within the bimolecular reaction) to rearrange equations (29). We get

$$\begin{aligned}
&(u-\mathcal{D})\frac{\mathrm{d}}{\mathrm{d}z}(n_1+n_3) + (n_1+n_3)\frac{\mathrm{d}u}{\mathrm{d}z} = 0 \\
&(u-\mathcal{D})\frac{\mathrm{d}}{\mathrm{d}z}(n_2+n_4) + (n_2+n_4)\frac{\mathrm{d}u}{\mathrm{d}z} = 0 \\
&(u-\mathcal{D})\frac{\mathrm{d}}{\mathrm{d}z}(n_1-n_2) + (n_1-n_2)\frac{\mathrm{d}u}{\mathrm{d}z} = 0 \\
&\frac{\mathrm{d}}{\mathrm{d}z}\left[(u-\mathcal{D})u\sum_i m_i n_i + \kappa T\sum_i n_i\right] = 0 \\
&\frac{\mathrm{d}}{\mathrm{d}z}\left\{(u-\mathcal{D})\left[u^2\sum_i m_i n_i + 3\kappa T\sum_i n_i + 2\sum_i E_i n_i\right] + 2\kappa T u\sum_i n_i\right\} = 0 \\
&(u-\mathcal{D})\frac{\mathrm{d}n_2}{\mathrm{d}z} + n_2\frac{\mathrm{d}u}{\mathrm{d}z} = S_1(n_1, \ldots, n_4, T).
\end{aligned} \tag{37}$$

The first five equations of (37) are conservation laws, while the sixth, generally called *rate equation* in the literature, takes into account production of species 2.

The first five equations can be formally integrated across the jump, namely from z_0 to $z \in (z_F, z_N)$. Recalling definitions (25) and that $u = 0$ in z_0, we obtain

$$\begin{aligned}
&(n_1+n_3)(u-\mathcal{D}) = -(n_{10}+n_{30})\mathcal{D} \\
&(n_2+n_4)(u-\mathcal{D}) = -(n_{20}+n_{40})\mathcal{D} \\
&(n_1-n_2)(u-\mathcal{D}) = -(n_{10}-n_{20})\mathcal{D} \\
&(u-\mathcal{D})u\sum_i m_i n_i + \kappa T\sum_i n_i = p_0 \\
&(u-\mathcal{D})\left[u^2\sum_i m_i n_i + 2\sum_i E_i n_i + 3\kappa T\sum_i n_i\right] + 2\kappa T u\sum_i n_i = -2(\mathcal{E}_0 + \mathcal{E}_{ch0})\mathcal{D}
\end{aligned} \tag{38}$$

where the subscript '0' denotes quantities computed in z_0.

From the first two relations we find

$$0 < u < \mathcal{D}$$

which is the detonation compatibility condition [3]. The set of equations (38) can be solved as a non-homogeneous algebraic system, expressing the unknowns n_1, n_3, n_4, u and T in terms of the progress variable n_2, where $\mathcal{D}$ is treated as a parameter. After some manipulations, we obtain for u the following two solutions:

$$u^{\pm}(n_2; \mathcal{D}) = \frac{2En_2 + 3\rho_0\mathcal{D}^2 - 5p_0 \pm \sqrt{\mathcal{P}(n_2; \mathcal{D})}}{8\rho_0\mathcal{D}} \tag{39}$$

where

$$\mathcal{P}(n_2; \mathcal{D}) = (2En_2 + 3\rho_0\mathcal{D}^2 - 5p_0)^2 - 32\rho_0 E\mathcal{D}^2(n_2 - n_{20}). \tag{40}$$

Accordingly, for the other unknowns we get

$$n_1^{\pm}(n_2; \mathcal{D}) = \frac{(n_{10} - n_{20})\mathcal{D}}{\mathcal{D} - u^{\pm}} + n_2 \tag{41}$$

$$n_3^{\pm}(n_2; \mathcal{D}) = \frac{(n_{20} + n_{30})\mathcal{D}}{\mathcal{D} - u^{\pm}} - n_2 \tag{42}$$

$$n_4^{\pm}(n_2; \mathcal{D}) = \frac{(n_{20} + n_{40})\mathcal{D}}{\mathcal{D} - u^{\pm}} - n_2 \tag{43}$$

$$T^{\pm}(n_2; \mathcal{D}) = \frac{(\mathcal{D} - u^{\pm})(\rho_0\mathcal{D}u^{\pm} + p_0)}{\kappa n_0\mathcal{D}} \tag{44}$$

with n_0 and ρ_0 defined by equations (18) and (19).

In order to obtain the rate equation for the unknown n_2, we plug expression (39) into the last equation of (37):

$$\frac{\mathrm{d}n_2^{\pm}}{\mathrm{d}z} = -\frac{8\rho_0\mathcal{D}S_1\left(n_2^{\pm}\right)}{\left[2En_2^{\pm} - 5\rho_0\mathcal{D}^2 - 5p_0 \pm \mathcal{Q}\left(n_2^{\pm}; \mathcal{D}\right)\right]\left[1 \pm \frac{2En_2^{\pm}}{\mathcal{Q}(n_2^{\pm}; \mathcal{D})}\right]} \tag{45}$$

where $\mathcal{Q} = \sqrt{\mathcal{P}}$. The signs $\pm$ in the last equation refer to solutions corresponding to u^+ and u^-, respectively. Moreover, $S_1\left(n_2^{\pm}\right)$ is given by expression (33) after substituting expressions (41)–(44) for $n_1^{\pm}$, $n_3^{\pm}$, $n_4^{\pm}$ and $T^{\pm}$.

Integration of equation (45) and computation of the other macroscopic observables (39) and (41)–(43) provide the physical state of the mixture in the reaction zone. According to the assumptions (36), this integration must be started at z_N with the initial datum

$$n_2^{\pm}(z_N) = n_{20} \tag{46}$$

and must be stopped when the right-hand side of equation (45) vanishes, that is when $n_2^{\pm}$ becomes constant since the reaction is completed and the gas reaches chemical equilibrium. Due to this condition, the corresponding coordinate z_F is found and the distance $|z_F - z_N|$ provides the thickness of the reaction zone. The final state of the reaction zone is then determined by computing $n_{iF} = n_i(z_F)$, $u_F = u(z_F)$ and $T_F = T(z_F)$. Such computations must be repeated for the explosive mixture for several $\mathcal{D}$ in order to find its minimum value capable to initiate detonation. As will be shown in section 6 this minimum value of $\mathcal{D}$ corresponds to the minimum value of u_F, which is obviously obtained when $\mathcal{P} \to 0$, that is $u_F^+ \to u_F^-$.

Let us now discuss the existence and physical consistence of the above solution (39)–(45). First, solutions to the detonation problem exist when $\mathcal{P} > 0$. On the other

hand, since $\mathcal{P}(n_2;\mathcal{D})$ is a convex parabola in the variable n_2, values of n_2 and the parameter $\mathcal{D}$ assuring positivity of $\mathcal{P}$ must exist.

Moreover, it can easily be shown that the solution corresponding to the values of u^- does not provide the expected jump in the point z_N. In fact, from explicit computations, recalling datum (46), the $\lim_{z\to z_N} u^-(n_2^-;\mathcal{D})$ vanishes $\forall\mathcal{D}$ and consequently also the quantities (41)–(44) with superscript '−' are continuous in z_0. Therefore, the unique non-trivial solution to the steady detonation problem is the one with the superscript '+' in equations (39)–(45). Thus, hereinafter, we will consider only the solution related to u^+, omitting the superscripts.

Regarding the physical consistency of the above solution, we can observe that positivity of T is evident. Moreover, since the choice of the two species 1 and 2 is free, hereinafter we will indicate with 2 the species that satisfies in region D_1 the condition $n_{10} > n_{20}$. Such a condition ensures positivity of n_1, while positivity of n_3 and n_4 in equations (42)–(43) implies that

$$n_2(z;\mathcal{D}) < \min\left[\frac{\mathcal{D}(n_{20}+n_{30})}{\mathcal{D}-u(z;\mathcal{D})}, \frac{\mathcal{D}(n_{20}+n_{40})}{\mathcal{D}-u(z;\mathcal{D})}\right].$$

In addition positivity of u is satisfied by

$$n_2(z;\mathcal{D}) > \frac{5p_0 - 3\rho_0\mathcal{D}^2}{2E}$$

so that the last two expressions provide upper and lower bounds for the progress variable in the reaction zone.

5. The Hugoniot diagram and the $\mathcal{D}$-discussion

This section provides all the detonation states achieved varying the parameter $\mathcal{D}$ at given initial conditions in region D_1. This, as widely discussed in [1, 2], can be achieved by constructing the Hugoniot diagram. To this end, we again consider equations (29)–(31) and let us rewrite them in the following way:

- multiplying equation (29) by m_i and summing over i results in

$$\frac{\partial\rho}{\partial t} + \frac{\partial}{\partial x}(\rho u) = 0 \tag{47}$$

  recalling that $\sum_i m_i S_i = 0$
- replacing the variable T in equation (30) with the hydrodynamic pressure $p = n\kappa T$:

$$\frac{\partial}{\partial t}(\rho u) + \frac{\partial}{\partial x}(\rho u^2 + p) = 0 \tag{48}$$

- introducing again $\mathcal{E}$ and $\mathcal{E}_{ch}$ in equation (31) yields

$$\frac{\partial}{\partial t}\left(\frac{1}{2}\rho u^2 + \mathcal{E} + \mathcal{E}_{ch}\right) + \frac{\partial}{\partial x}\left[u\left(\frac{1}{2}\rho u^2 + p + \mathcal{E} + \mathcal{E}_{ch}\right)\right] = 0. \tag{49}$$

Let us now apply transformation (34) to these last three equations and integrate formally from $z_0 \in D_1$ to any point z in the reaction zone. We get

$$\begin{aligned} &\rho(\mathcal{D}-u) = \rho_0\mathcal{D} \qquad\qquad \rho u(\mathcal{D}-u) - p = -p_0 \\ &(\mathcal{D}-u)\left(\tfrac{1}{2}\rho u^2 + \mathcal{E} + \mathcal{E}_{ch}\right) - up = \mathcal{D}(\mathcal{E}_0 + \mathcal{E}_{ch0}) \end{aligned} \tag{50}$$

recalling that in D_1 we have set $u_0 = 0$.

By eliminating the quantity u from the first and second equations of (50) and introducing the specific volume $v = 1/\rho$, we obtain

$$p = p_0 - \rho_0^2 \mathcal{D}^2 (v - v_0). \tag{51}$$

The last equation is the Rayleigh line of slope $-\rho_0^2\mathcal{D}^2$ in the plane (v, p). Analogously, by eliminating the variables u and $\mathcal{D}$ from equations (50), we get

$$\frac{1}{2}(v_0 - v)(p + p_0) = \frac{1}{\rho}(\mathcal{E} + \mathcal{E}_{ch}) - \frac{1}{\rho_0}(\mathcal{E}_0 + \mathcal{E}_{ch0}) \tag{52}$$

which is known as the Hugoniot equation in the plane (v, p). Equations (51) and (52) are the same equations that rule detonation in classical macroscopic theory. A more interesting form of the Hugoniot equation (52) can be deduced to draw the Hugoniot diagram. Taking into account relation (25), the internal energy per unit mass $\mathcal{E}/\rho$ can be expressed in terms of v and p, i.e. $\mathcal{E}/\rho = (3/2)vp$, and then rearranged together with the left-hand side of equation (52). Now, the Hugoniot equation becomes

$$\left(v - \frac{v_0}{4}\right)\left(p + \frac{p_0}{4}\right) = \frac{q}{2} + \frac{15}{16} v_0 p_0 \tag{53}$$

where $q = \mathcal{E}_{ch0}/\rho_0 - \mathcal{E}_{ch}/\rho$ can be expressed through definition (25) and equations (41)–(43) at every point z of the reaction zone for a given initial state and a fixed $\mathcal{D}$ in terms of the progress variable $n_2(z)$ and the mean velocity $u(z)$, i.e.

$$q(z) = \frac{E}{\rho_0}\left[\frac{\mathcal{D} - u(z)}{\mathcal{D}} n_2(z) - n_{20}\right]. \tag{54}$$

Therefore, to compute $q(z)$, it is necessary to integrate equation (45).

Equation (53) represents a sheaf of rectangular hyperbola in the plane (v, p) centred at the point $(v_0/4, -p_0/4)$ with q as a parameter. For an assigned propagation velocity $\mathcal{D}$, the detonation state itself is obtained at one of the two intersections between the Hugoniot curve and the related Rayleigh line. To understand which one is the intersection point that corresponds to the actual solution of the detonation problem, we consider the Hugoniot curve computable through the quantity $q_F = q(z_F)$ in the final point z_F of the reaction zone. For this hyperbola, it is possible to define the Rayleigh line with slope $-\rho_0^2\mathcal{D}_J^2$ which is tangent to the hyperbola itself in the point J. The quantity $\mathcal{D}_J$ is known in the literature as the Chapman–Jouguet velocity. The point J divides the Hugoniot curve into two parts: the *weak branch* below and the *strong branch* above. All the intersection points of the strong branch are the actual solutions of the detonation problem (see [2]), and this will be verified numerically in the next section.

Finally, let us note that by imposing the tangency condition between the line equation (51) and the curve equation (53), it is possible to recover the expression of $\mathcal{D}_J$ and of the coordinates of the point J in the (v, p) plane. After some algebra one obtains

$$\mathcal{D}_J = \sqrt{\frac{15p_0 + 16\rho_0 q_F + 4\sqrt{2\rho_0 q_F(8\rho_0 q_F + 15p_0)}}{9\rho_0}} \tag{55}$$

and

$$v_J = \frac{5}{8}\left(v_0 + \frac{p_0}{\rho_0^2 D_J^2}\right) \qquad p_J = \frac{3}{8}\left(p_0 + \rho_0 D_J^2\right). \tag{56}$$

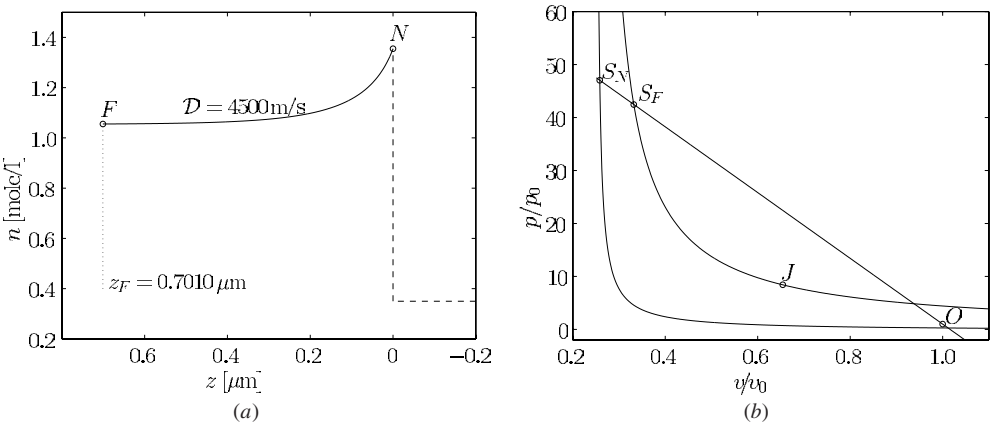

Figure 2. Total number density n versus z in the reaction zone (N, F) for $\mathcal{D} = 4500$ m s^{-1} (a). Corresponding Hugoniot diagram (b): the points on the Rayleigh line between S_N and S_F denote the detonation states in the reaction zone. The initial state is indicated by O and the Chapman–Jouguet point by J.

6. Numerical results

In this section, we show some numerical simulations to describe the detonation structure. The simulations regard the following chemical reaction

$$H_2O + H \rightleftharpoons OH + H_2$$

for which the heat of reaction $E = 63.3$ kJ/mole and the threshold for the exothermic reaction $E_A = 13.8$ kJ/mole is linked via

$$\chi = \sqrt{\frac{2E_A}{\mu_{34}}}$$

to $\chi = 3927$ m s^{-1}. The chosen constant $\beta = 10^9$ l/mole s that scales the cross section (8), corresponds to the Arrhenius parameters of the considered reaction.

By numerically integrating equation (45), starting from the initial datum n_{20}, and using equations (39) and (41)–(44) we are able to recover all the macroscopic quantities of the system from the Von Neumann point of coordinate z_N to the final point z_F. In figure 2(a), we plot the profile of the total number density n versus z in the reaction zone for a fixed value of $\mathcal{D} =$ 4500 m s^{-1} and for the following values of the macroscopic quantities in the unperturbed region D_1: $n_{10} = 0.03$ mole l^{-1}, $n_{20} = 0.02$ mole l^{-1}, $n_{30} = 0.1$ mole l^{-1}, $n_{40} =$ 0.2 mole l^{-1} and $T_0 = 298.15$ K. By varying $\mathcal{D}$ in this simulation, it turns out that the minimum value allowing existence of a solution is $\mathcal{D} = 3110$ m s^{-1}. The coordinate z_F which marks the thickness of the reaction zone is defined in the numerical computations by the minimum value of the variable z for which the difference of two consecutive particle densities $n_2(z)$ and $n_2(z + \Delta z)$ is less than 10^{-5} mole l^{-1}. We fixed Δz as 5×10^{-10} m. In figure 2(b), we represent the same results in the Hugoniot plane $(v/v_0,\ p/p_0)$. We plot two of the Hugoniot hyperbolae: the lower one for $z = z_N$ and the upper one for $z = z_F$. The detonation states in the reaction zone are all the points of the Rayleigh line (for the chosen value of $\mathcal{D}$) between S_N and S_F. Moreover, we draw the Chapman–Jouguet point J and the initial state O. It should be noted that the solution lays on the strong branch above J.

Figures 3(a)–(c) present a parameter study showing how the speed of the shock wave $\mathcal{D} = 3500$, 4000 and 4500 m s^{-1} affects the macroscopic state variables n, T and u in and the

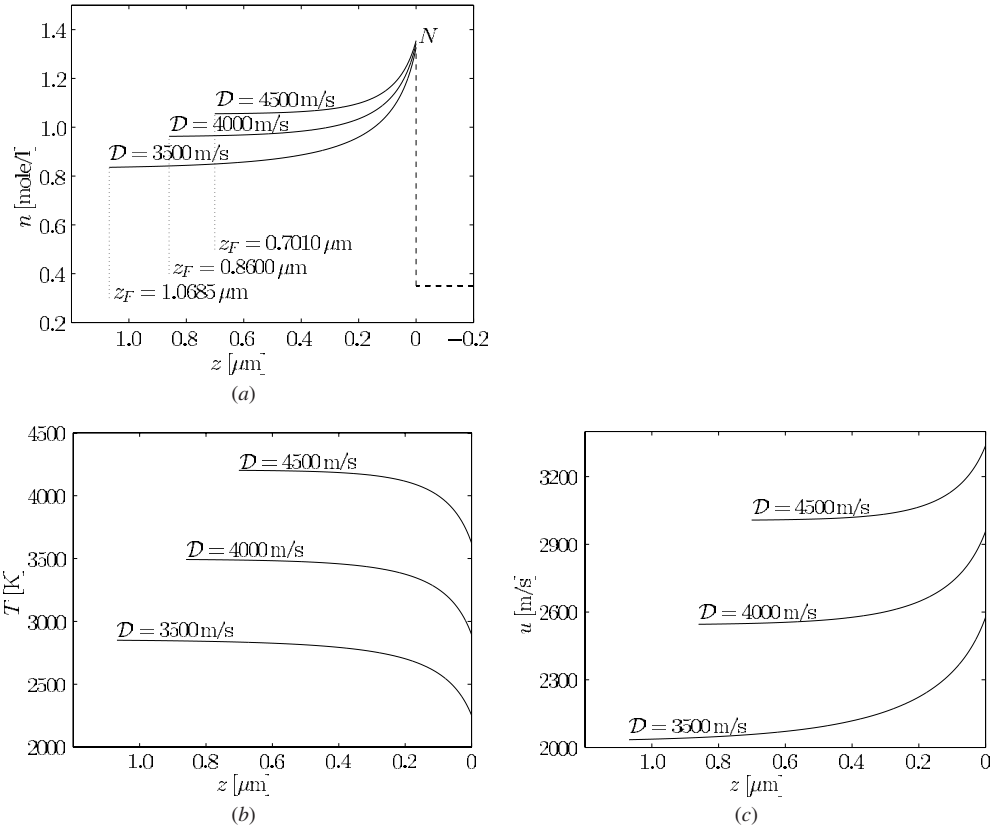

Figure 3. Total number density n (a), temperature T (b) and mean velocity u (c) in the reaction zone for several shock wave speeds.

thickness of the reaction zone, respectively. We observe an approximately linear increase of the temperature profiles (figure 3(b)), whereas the thickness of the reaction zone (figure 3(a)) decreases nonlinearly for increasing speed of the shock wave. This behaviour is expected on physical grounds. The higher the speed of the shock and consequently the temperature in the reaction zone, the faster the reaction runs because increasingly more particles are able to overcome the threshold energy necessary to undergo a chemical reaction. In addition, due to the mass action law, the chemical equilibrium is shifted due to the increasingly higher temperature, which results again in a reduction of the reaction zone. It is also plausible that according to higher temperature profiles with increasing shock wave speeds, we have to expect an increase for the bulk velocity u as shown in figure 3(c). It should be noted that these results are in good agreement, qualitatively and, at least, for the order of magnitude of observables, with those reported in [1, 2]. This matter will be discussed in the next section.

The developed model also reflects the influence of the energy threshold on the physical state variables. To demonstrate this effect regarding the total number density n, we recompute the profiles in figure 3(a) by assuming E_A to be 2.0 kJ/mole. The comparison of the results in figure 4 with those in figure 3(a) reveals that the reaction zone becomes shorter in the case of a lower threshold.

Finally, we show with figure 5 that a maximum value for the thickness of the reaction zone with respect to the speed of the shock wave exists. This maximum is located close to the minimum value of $\mathcal{D}$.

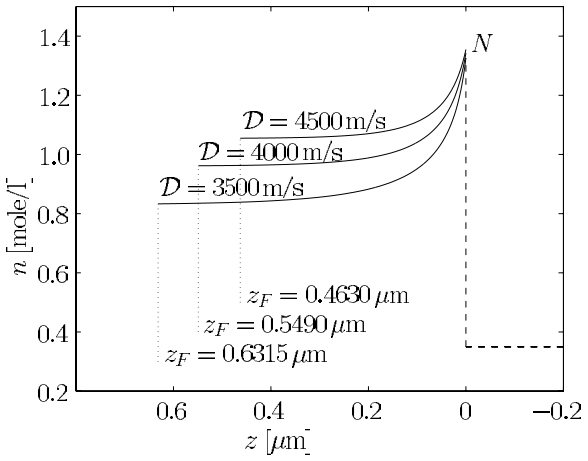

Figure 4. Total number density n and thickness of the reaction zone z_F calculated for a small threshold energy $E_A = 2$ kJ/mole and several shock wave speeds.

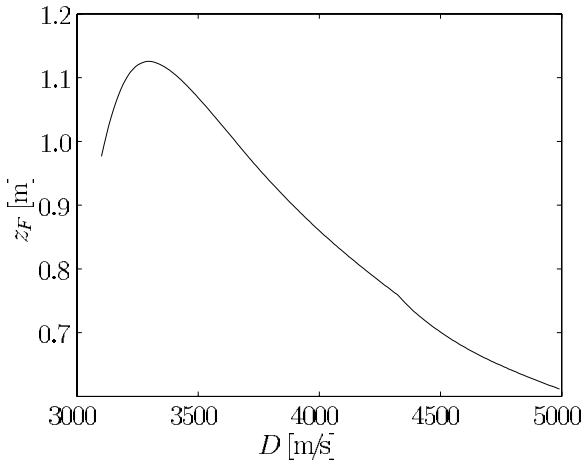

Figure 5. Thickness of the reaction zone z_F versus the speed of the shock wave $\mathcal{D}$.

7. Concluding remarks

The aim of this paper is to provide an accurate analysis of the profiles of macroscopic quantities in the so-called reaction zone, which follows the steady shock propagation due to a detonation process. In more detail, such an analysis allows us to calculate the thickness of the reaction zone for finding the coordinate z_F, where the zone ends and the chemical disequilibrium due to the entire process of detonation disappears. Moreover, the analysis carried on in the paper also allows us to evaluate the minimum value of the detonation velocity for which the detonation itself occurs.

In the authors' opinion, to pursue the mentioned objectives, it is convenient to set the detonation problem at a microscopic scale describing the physical system via a Boltzmann equation, which takes into account the class of chemical reactions driving the process. The main advantage of this choice consists, as shown in section 3, in recovering in a rigorous way

the equations governing the process at the macroscopic scale and providing at the same time an accurate analytical expression of the reaction rate.

Moreover, in section 4 we propose a computational method capable of providing the aforementioned profiles in the reaction zone, almost all in analytical form. This requires only the numerical solution to a boundary-value problem governed by a single ODE. In addition, by using the Hugoniot diagram (see section 5), such a solution represented in the (v, p) plane allows us to evaluate the value of the so-called Chapman–Jouguet velocity, which is the minimum value of the detonation velocity assuring the existence of a steady detonation at a given physical state of the gas mixture in the unperturbed region.

In section 6, we present some numerical results showing profiles of number density, temperature and mean velocity versus z in the reaction zone. These results are then reported in the (v, p) plane. Moreover, we also provide the thickness of the reaction zone as a function of the detonation velocity.

As discussed in section 1, these results cannot be easily compared to other theoretical results. Nevertheless, on a qualitative ground, they are very similar to those obtained by using a Monte Carlo method, which have been presented in the two recent papers [17, 18]. In fact, these authors and those of papers [19, 20], which are mainly concerned with stability problems, consider chemical reactions as responsible for ultrafast or pathological detonations, such as $A + M \rightarrow B + M$, M being alternatively A or B, and $A \rightarrow B \rightarrow C$ (the former exothermic, the latter endothermic). Therefore, quantitative comparisons with the reactions of the present paper are not possible.

As already anticipated in section 1, the method proposed here can be applied to reactions other than bimolecular ones, which drive detonations, as for instance those of dissociation/recombination for which a forthcoming paper is in preparation.

In fact, most of the experimental results presented in the literature are concerned with detonations driven by dissociation reactions. These results can be found in [1, 2] and several papers, as for instance, the very recent one [37], where dissociation of the system H_2–Cl_2 is considered. In general, in these experiments quantities relevant to the entire process of detonation are not measured, since the observation is limited to the so-called detonability conditions, i.e. the determination of the propagation velocity of the shock and the values of macroscopic observables on its edge in terms of the physical state of the gas in the unperturbed region.

Of course in this paper, as in all the papers quoted here, the detonation process is somehow idealized through a description in 1D. Many experimental results and measurements are nowadays documented as pattern formation in 2D. Consequently, a natural improvement of the present theory, hopefully comparable with experiments, should be developed in more than one dimension.

References

[1] Glassman I 1996 *Combustion* (San Diego: Academic)
[2] Kuo K K 1986 *Principles of Combustion* (New York: Wiley)
[3] Fickett W 1986 *Introduction to Detonation Theory* (Berkeley, CA: University of California Press)
[4] Fickett W and Davis W C 1979 *Detonation* (Berkeley, CA: University of California Press)
[5] Majda A 1981 A qualitative model for dynamic combustion *SIAM J. Appl. Math.* **41** 70–93
[6] Rosales R R and Majda A 1983 Weakly nonlinear detonation waves *SIAM J. Appl. Math.* **43** 1086–118
[7] Lombardo S and Torrisi M 1994 On some special classes of similarity solutions of the Wood–Kirkwood model in detonation theory *Int. J. Eng. Sci.* **32** 669–80
[8] Gasser I and Szmolyan P 1995 Detonation and deflagration waves with multistep reaction schemes *SIAM J. Appl. Math.* **55** 175–91

[9] Liu T P and Ying L A 1995 Nonlinear stability of strong detonations for a viscous combustion model *SIAM J. Math. Anal.* **26** 519–28
[10] Schmitt R G and Butler P B 1995 Detonation-wave structure of gases at elevated initial pressures *Combust. Sci. Technol.* **107** 355–85
[11] Clavin P and He L T 1996 Stability and nonlinear dynamics of one-dimensional overdriven detonations in gases *J. Fluid Mech.* **306** 353–78
[12] Li D, Liu T P and Tan D 1996 Stability of strong detonation travelling waves to combustion model *J. Math. Anal. Appl.* **201** 516–31
[13] Tegnér J K 1996 Properties of detonation waves *Math. Methods Appl. Sci.* **19** 1279–301
[14] Short M 1997 On the critical conditions for the initiation of a detonation in a nonuniformly perturbed reactive fluid *SIAM J. Appl. Math.* **57** 1242–80
[15] Tan D and Tesei A 1997 Nonlinear stability of strong detonation waves in gas dynamical combustion *Nonlinearity* **10** 355–76
[16] Bebernes J and Eberly D 1989 *Mathematical Problems from Combustion Theory (Springer Applied Mathematical Sciences)* (New York: Springer)
[17] Anderson J B and Long N L 2003 Direct Monte Carlo simulation of chemical reaction systems: prediction of ultrafast detonations *J. Chem. Phys.* **118** 3102–10
[18] Anderson J B and Long N L 2003 Direct simulation of pathological detonation *Proc. 23rd Int. Symp. on Rarefied Gas Dynamics (Whistler)* at press
[19] Sharpe G J 1999 Linear stability of pathological detonations *J. Fluid Mech.* **401** 311–38
[20] Sharpe G J and Falle S 2000 One-dimensional nonlinear stability of pathological detonations *J. Fluid Mech.* **414** 339–66
[21] Monaco R, Pandolfi Bianchi M and Soares A J 1996 Steady detonation waves in classical and discrete kinetic theory *Commun. Appl. Nonlinear Anal.* **3** 1–19
[22] Pandolfi Bianchi M and Soares A J 1996 A kinetic model for a reactive gas flow: steady detonation and speeds of sound *Phys. Fluids* A **8** 3423–32
[23] Pandolfi Bianchi M and Soares A J 2000 Kinetic formulation of linear stability for steady detonation waves *Riv. Mat. Univ. Parma* **3** 85–106
[24] Rossani A and Spiga G 1999 A note on the kinetic theory of chemically reacting gases *Physica* A **272** 563–73
[25] Griehsnig P, Schürrer F and Kügerl G 1992 Kinetic theory for particles with internal degrees of freedom *Rarefied Gas Dynamics: Theory and Simulations* vol 159, ed B D Shizgal and D P Weaver (Washington: AIAA) pp 581–9
[26] Koller W and Schürrer F 2001 Conservative solution methods for extended Boltzmann equations *Riv. Mat. Univ. Parma* **4*** 109–69
[27] Polewczak J 2001 A review of the kinetic modelings for non-reactive and reactive dense fluids: questions and problems *Riv. Mat. Univ. Parma* **4*** 23–55
[28] Ross J, Light J C and Schuler K E 1969 Rate coefficients, reaction cross sections and microscopic reversibility *Kinetic Processes in Gases and Plasmas* ed A R Hochstim (New York: Academic) pp 281–320
[29] Levine R D and Bernstein R B 1987 *Molecular Reaction Dynamics and Chemical Reactivity* (New York: Oxford University Press)
[30] Present R D 1959 On the velocity distribution in a chemically reacting gas. *J. Chem. Phys.* **31** 747–50
[31] Greene E F and Kuppermann A 1968 Chemical reaction cross sections and rate constants. *J. Chem. Educ.* **45** 361–9
[32] Kogan M N 1969 *Rarefied Gas Dynamics* (New York: Plenum)
[33] Garibotti C R and Spiga G 1994 Boltzmann equation for inelastic scattering. *J. Phys. A: Math. Gen.* **27** 2709–21
[34] Weissbacher B 1999 BGK-approach to kinetic equations of chemically reacting gases *Diploma Thesis* Graz University of Technology, Graz, Austria
[35] Yeremin E N 1979 *The Foundations of Chemical Kinetics* (Moscow: MIR)
[36] Cercignani C 1988 *The Boltzmann Equation and its Applications* (New York: Springer)
[37] Dionne J P, Duquette R, Yoshinaka A and Lee J H S 2000 Measurements of pathological detonations in H_2–Cl_2 dissociation *Combust. Sci. Technol.* **158** 5–14